

# Advancing the Frontier of Meteorological Sensing: A Detailed Performance Analysis of the TempVue™20

Paul Bartosek, Atefeh Hosseini, Alex Thomas, Campbell Scientific, Inc.

## Introduction

The TempVue™20 temperature sensor is designed for high-accuracy measurement in demanding environmental applications. This study presents the results of a controlled uncertainty testing campaign evaluating the TempVue 20's performance across an extreme temperature range (–60 to +60°C). Using a high-precision platinum resistance thermometer (PRT) as the reference standard, the study assessed measurement accuracy, repeatability, and statistical confidence in compliance with internal specifications and internationally recognized standards. Results demonstrate that the TempVue 20 exceeds one-third of the Class B (Class W0.1 or F0.1) specifications across the full tested temperature range, consistently delivering precise and reliable measurements, and confirming its suitability for critical monitoring environments.

## Raising the Bar in Environmental Sensing

Environmental monitoring systems increasingly demand sensors that can perform reliably under extreme conditions. Whether deployed in arctic research stations or desert meteorological networks, accuracy and consistency in temperature measurements are critical to data integrity.

The TempVue 20 is built to meet that challenge. At its core is a wire-wound, four-wire Pt100 resistance temperature detector (RTD) element, encapsulated in a slim, stainless-steel probe housing filled with thermal epoxy. This design provides exceptional response time while protecting against mechanical and thermal stress. The sensor meets World Meteorological Organization (WMO) standards, achieving a 20-second step response at an ambient wind speed of just 1 m/s (3.3 ft/s). Unlike traditional analog sensors, the TempVue 20 operates digitally, providing status diagnostics, streamlining system integration, and eliminating calibration uncertainty. It also minimizes self-heating by employing short excitation periods (tens of milliseconds) and a very low operating current (–250 µA). Most importantly, the TempVue 20 surpasses one-third of Class B accuracy requirements (Class W0.1 or F0.1), achieving a maximum uncertainty of only 0.3 K across –60 to +60°C, and as low as 0.1 K within –40 to +40°C, the temperature range most relevant to meteorological applications.

But how does it perform in practice?

## Testing Methodology

To evaluate the TempVue 20's accuracy, a total of 24 units were tested in a temperature-controlled environmental chamber alongside a high-precision reference sensor. The reference was a Class A standard PRT (SPRT), JMS Southeast Model 3SSBNK6BZZ3(80) HWZA8. The JMS probe is a 1/10 DIN probe with a widely accepted measurement uncertainty of  $\pm 0.03^{\circ}\text{C}$ . For comparison, measurement results were evaluated against multiple specifications: the TempVue maximum allowed error, Class A tolerance, 1/3 Class B specification, and 1/10 Class B specification.

Sensor readings were collected every 15 seconds using a synchronized scan cycle. The test protocol involved two distinct phases:

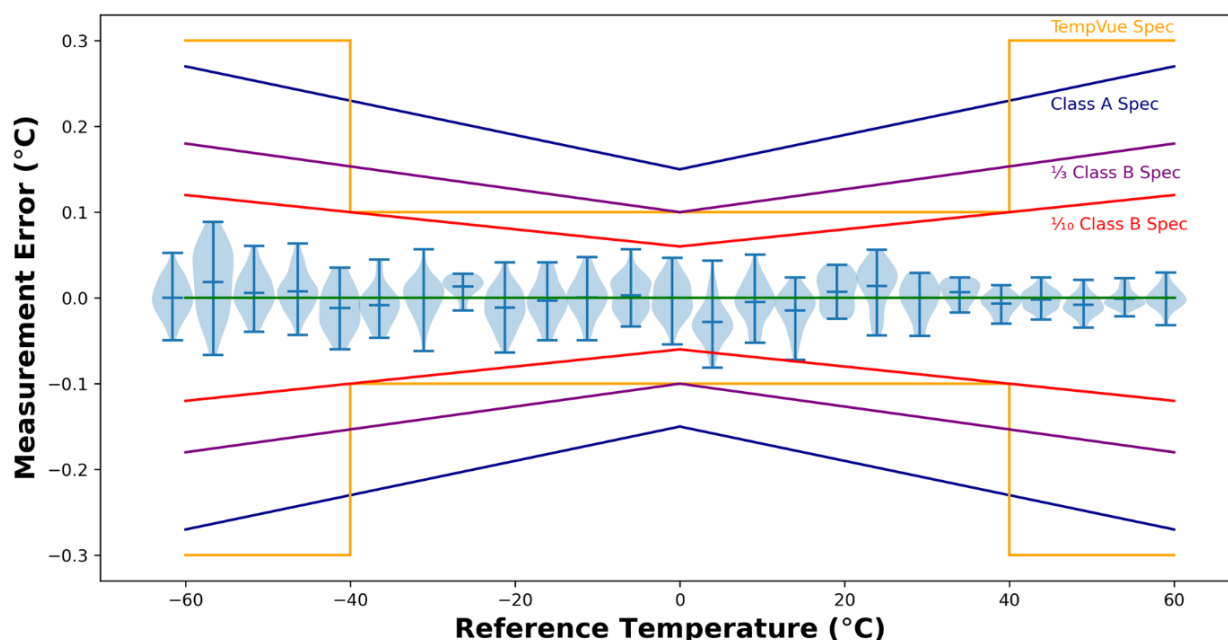
- **Cool-Down Phase:** The chamber was ramped down to  $-60^{\circ}\text{C}$  and held at that temperature for 30 minutes to ensure thermal equilibrium.
- **Stepwise Heating Phase:** The chamber temperature increased in  $5^{\circ}\text{C}$  increments, with each new setpoint maintained for 15 minutes. This process continued until a final temperature of  $+60^{\circ}\text{C}$  was reached. Data acquisition for the measurement began once the device under test (DUT) temperature standard deviation fell below  $0.01^{\circ}\text{C}$  for 12 consecutive samples (60 seconds).

At each dwell point, temperature readings (DUTs) from all 24 TempVue 20 sensors were compared against the reference thermometer. The measurement error for each DUT was calculated as the difference between its reading and the reference. These errors were visualized as vertical histograms for each temperature step, illustrating the distribution and consistency of the sensor deviations across the test range.

## Results: Accuracy and Confidence

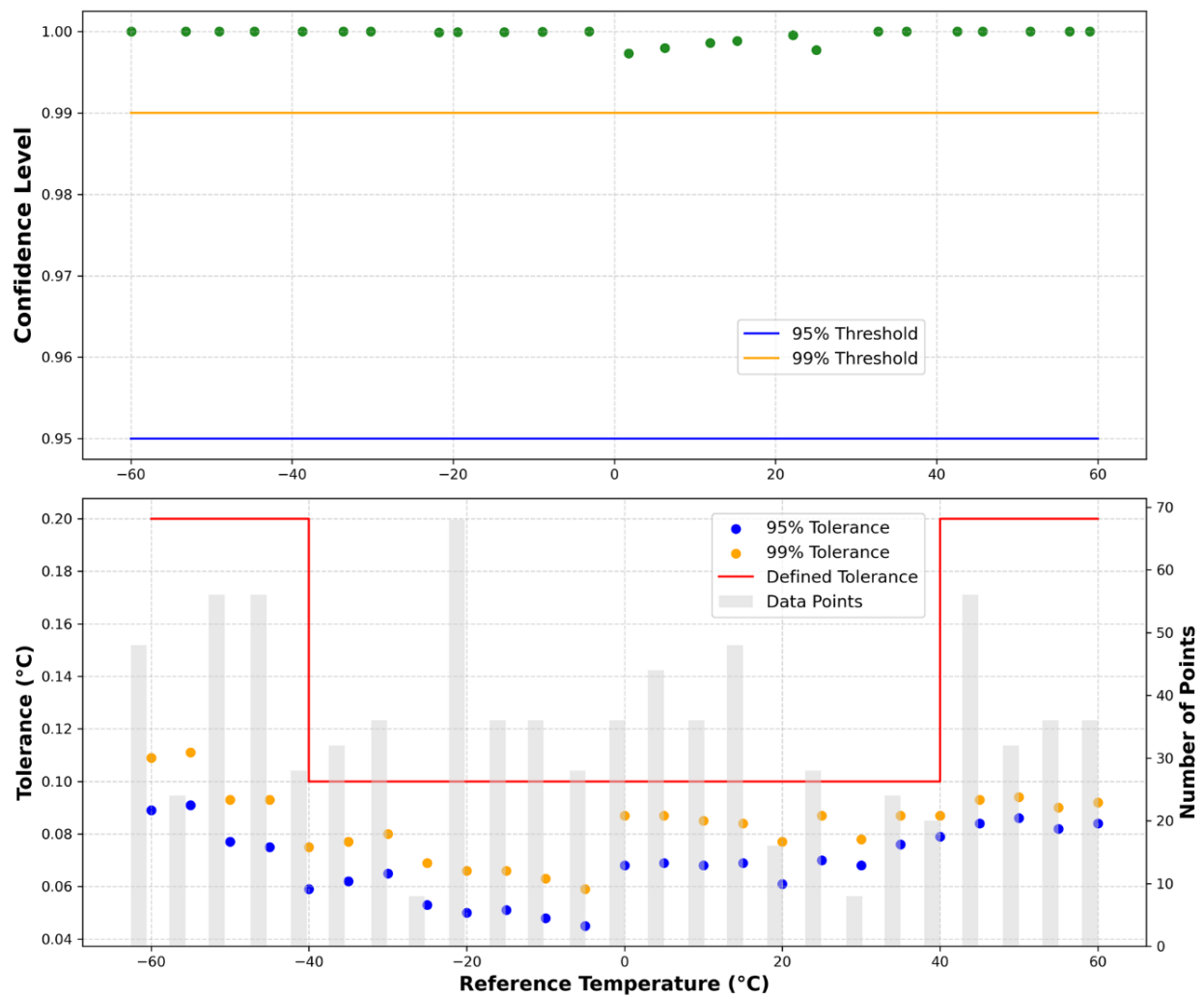
The results and performance evaluation, as presented in Figure 1, illustrate the measurement error, defined as the difference between each TempVue 20 sensor reading and the reference temperature. Figure 1 shows the distribution of measurement errors for all 24 TempVue 20 sensors at each temperature step. The blue violin plots depict the spread and density of these errors. For comparison, several tolerance limits are included.

At  $5^{\circ}\text{C}$ , the TempVue 20's measurement error distribution approaches the limits of the stringent 1/10 Class B tolerance. The tails of the blue violin plot indicate that a small fraction of sensor readings slightly exceed the red lines representing this tolerance, suggesting that while most measurements are highly accurate, a few do not fully meet this exceptionally tight requirement. For all other specifications—including the 1/3 Class B, IEC Class A, and the device's own design tolerance of  $\pm 0.1^{\circ}\text{C}$ —the sensor errors remain well within the bounds, demonstrating strong performance across all but the most demanding standards at this temperature.



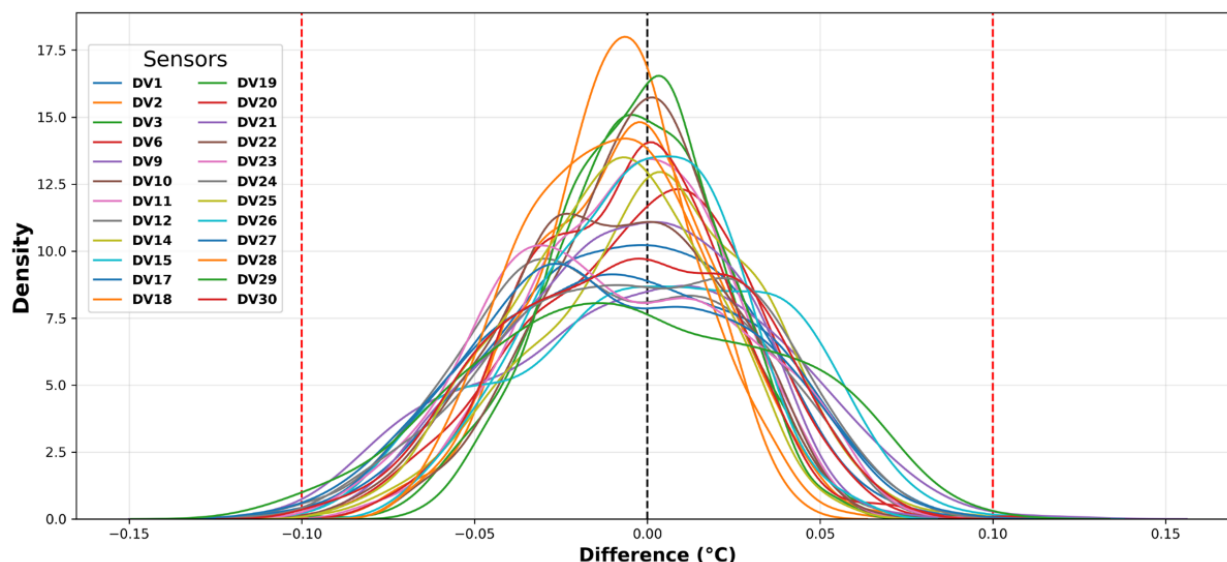
**Figure 1:** Measurement error distributions for 24 TempVue 20 sensors (blue violins) relative to a reference thermometer across  $-60$  to  $+60^{\circ}\text{C}$ . The green line represents zero error. Several tolerance specifications are included for comparison: the orange lines indicate the TempVue 20 design specifications ( $\pm 0.1^{\circ}\text{C}$  within  $-40$  to  $+40^{\circ}\text{C}$  and  $\pm 0.3^{\circ}\text{C}$  outside this range); the blue lines show IEC 60751 Class A limits; the purple lines denote  $1/3$  Class B tolerance; and the red lines correspond to the stringent  $1/10$  Class B tolerance.

Figure 2 presents a comprehensive statistical analysis of TempVue 20 sensor conformance. The top panel shows confidence levels near 100% across nearly all temperature steps, indicating that all 24 units consistently met specifications over the  $-60$  to  $+60^{\circ}\text{C}$  range. The bottom panel depicts the observed proportion of out-of-specification sensors against 95% and 99% confidence thresholds, with all data points remaining well below the maximum allowable limits, approximately  $0.1^{\circ}\text{C}$  between  $-40$  and  $+40^{\circ}\text{C}$ , and  $0.3^{\circ}\text{C}$  outside this range.



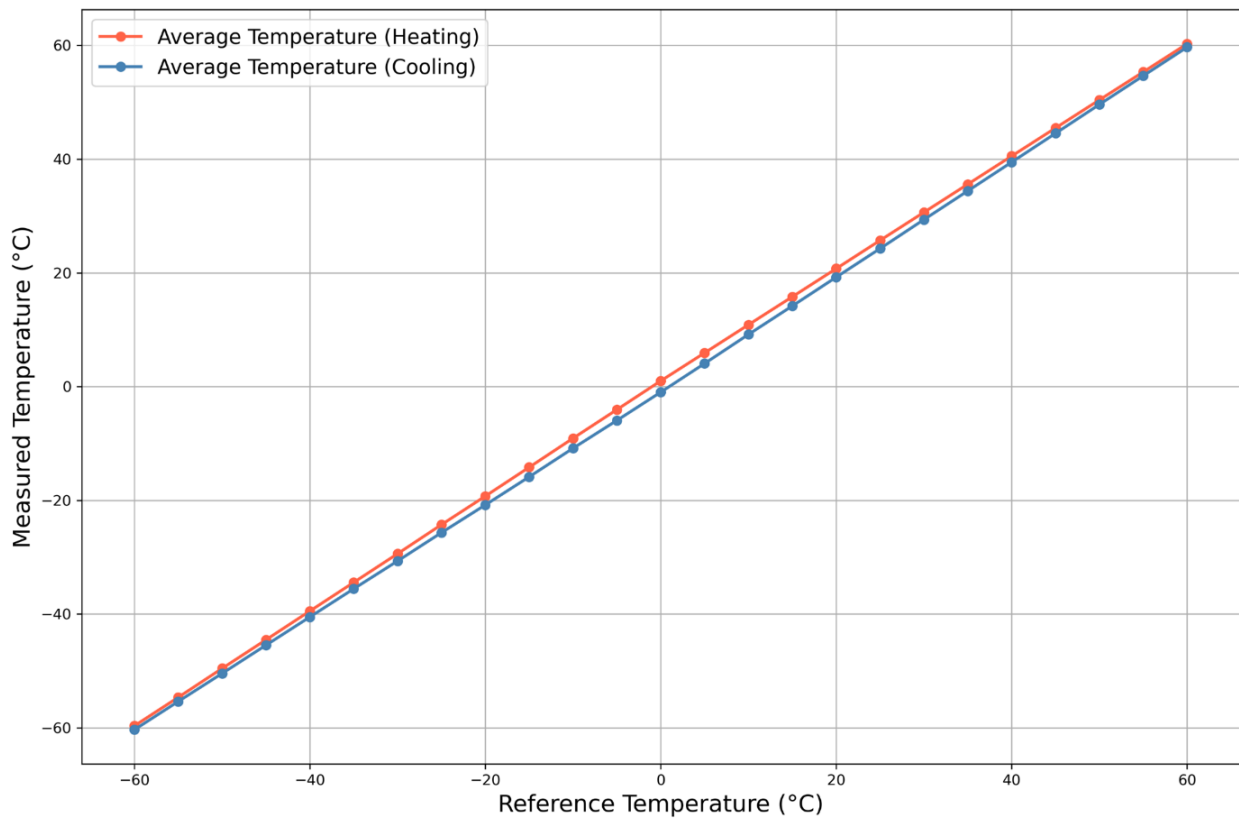
**Figure 2:** Statistical analysis of TempVue 20 compliance. The top panel shows confidence levels near 100% against 95% (orange) and 99% (blue) benchmarks. The bottom panel plots observed out-of-spec tolerance at 95% (blue) and 99% (orange) confidence within binomial bounds (red), confirming robust adherence to  $\pm 0.1^{\circ}\text{C}$  ( $-40$  to  $+40^{\circ}\text{C}$ ) and  $\pm 0.3^{\circ}\text{C}$  (outside) limits. The gray bars represent the number of data points collected at each reference temperature.

Figure 3 shows the density functions of the differences between each DUT and the corresponding standard value, based on all 24 sensor measurements at each time step for measurements between  $-40$  and  $40^{\circ}\text{C}$ . Each colored curve represents an individual DUT, with its shape reflecting the device's performance characteristics. Overall, all devices operate within the specified acceptance range, indicated by the red dashed lines at  $\pm 0.1^{\circ}\text{C}$ . Devices with tall, narrow peaks near  $0.0^{\circ}\text{C}$  exhibit high precision and low variability, whereas flatter, broader distributions indicate greater variability, even when measurements remain within the acceptable range.



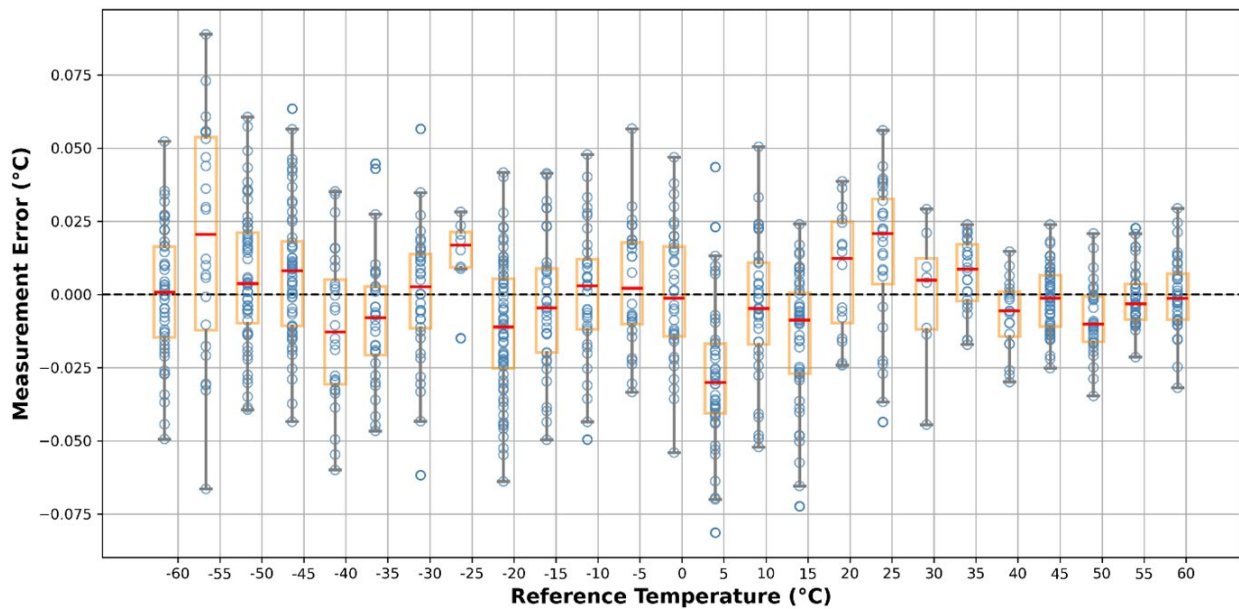
**Figure 3:** Probability density functions of DUT difference from reference value. The central black line at 0.0°C represents perfect agreement, while the red dashed lines at  $\pm 0.1^\circ\text{C}$  indicate the maximum allowable limits within the  $-40$  to  $+40^\circ\text{C}$  range.

Hysteresis is calculated by comparing sensor measurements during heating and cooling cycles. Heating progresses from  $-60$  to  $+60^\circ\text{C}$ , while cooling descends from  $+60$  to  $-60^\circ\text{C}$ , with a small hysteresis offset added to the simulated data to model the tendency of sensors to read slightly higher during heating and slightly lower during cooling. The data are separated into heating and cooling segments. The average, standard deviation, minimum, and maximum readings across all devices are calculated at each reference temperature. Hysteresis at each point is quantified as the difference between the average heating and cooling measurements, with the resulting gap visually representing the effect. Figure 4 shows the sensor's hysteresis behavior, where the heating and cooling curves illustrate a small but measurable effect. The heating curve (red) consistently registers slightly higher temperatures than the cooling curve (blue) at the same reference points. This effect is most pronounced around  $\pm 10^\circ\text{C}$ , with the maximum difference near  $0^\circ\text{C}$ .



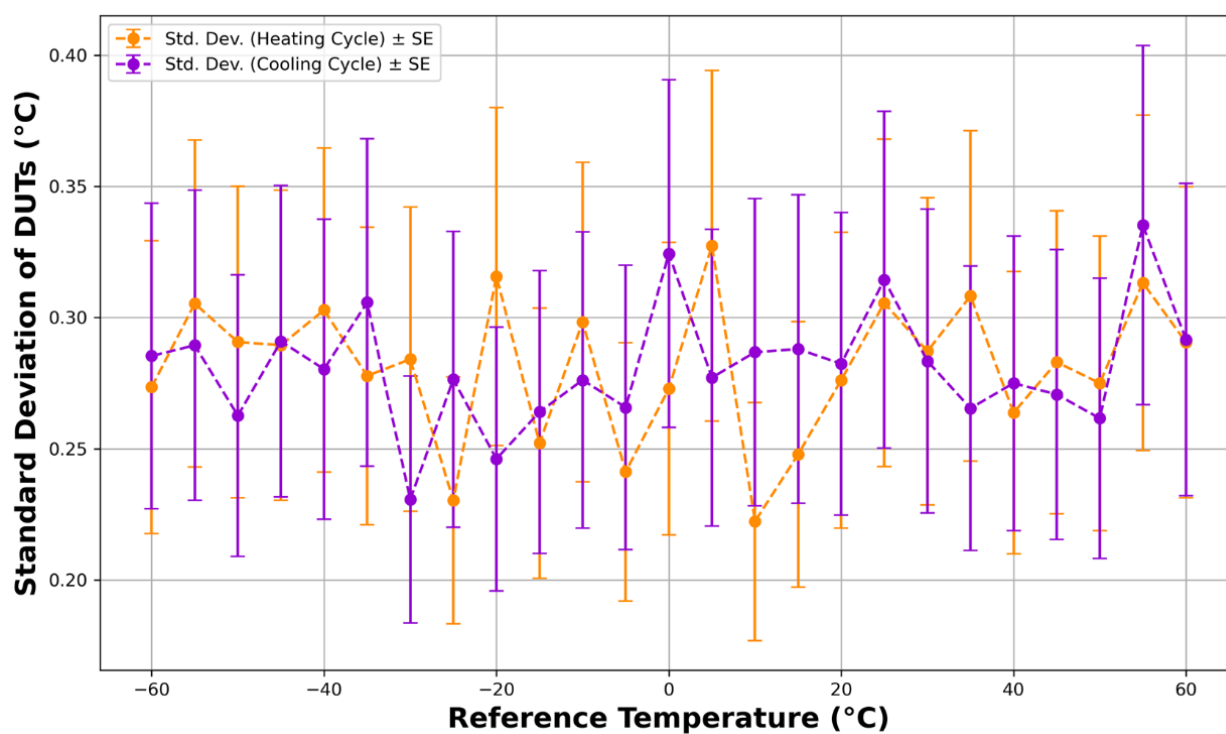
**Figure 4:** Hysteresis behavior of the sensor. Heating (red) and cooling (blue) curves across the  $-60$  to  $+60^{\circ}\text{C}$  range.

Figure 5 presents the sensor data as individual points (blue circles) overlaid on box plots. Across most of the temperature range, the spread is roughly symmetric around the mean error (red line), although it increases slightly near the extremes ( $-60$  and  $+60^{\circ}\text{C}$ ), indicating higher noise at the sensor's operational limits. Ideally, the mean measurement error would remain zero across all temperatures; however, small systematic deviations are observed at specific points (e.g.,  $-55^{\circ}\text{C}$ ,  $-20^{\circ}\text{C}$ , and  $+25^{\circ}\text{C}$ ), reflecting minor nonlinearity.



**Figure 5:** Distribution of sensor measurement errors across reference temperatures. Individual measurements are shown as blue dots, while boxplots summarize the median, interquartile range, and overall variability.

Figure 6 shows the standard deviation calculated across all measurements from all DUTs at each temperature step, rather than as an average of individual DUT standard deviations. Over the full temperature range, it generally varies between +0.20 and +0.35°C, with no noticeable increase in noise at the extremes (–60 and +60°C).



**Figure 6:** Standard deviation of DUT measurements at each temperature as a function of the reference temperature. The orange line represents the heating cycle and the purple line represents the cooling cycle. Error bars indicate the standard error (SE) across the 24 DUTs.

## Conclusion

Across the full  $-60$  to  $+60^{\circ}\text{C}$  range, the TempVue 20 exhibited consistently high measurement accuracy, minimal bias, and strong repeatability. Measurement errors were tightly clustered around zero and remained well within internal design specifications as well as IEC 60751 Class A, 1/3 Class B, and 1/10 Class B limits (Figure 1). Confidence analysis confirmed that all 24 tested units met specification thresholds with near-complete compliance across all temperature steps (Figure 2), underscoring the sensor's reliability and robust, calibration-free design.

Although the sample size was modest ( $n = 24$ ), these results provide strong initial evidence of the TempVue 20's suitability for precise, low-maintenance temperature monitoring in harsh environmental conditions. The minimal separation between heating and cooling curves (Figure 3) indicates low thermal lag and demonstrates the sensor's rapid and efficient response to temperature changes. Observed hysteresis, typical of high-precision temperature sensors, likely arises from intrinsic properties of the sensing element or the surrounding system, including thermal inertia and energy dissipation. Overall, the small magnitude of hysteresis confirms that the sensor provides reliable and repeatable measurements across the tested temperature range.



Analysis of the density function of all DUTs within  $\pm 40^{\circ}\text{C}$  (Figure 4) shows that all devices operate within the specified acceptance range, indicated by the red dashed lines at  $\pm 0.3^{\circ}\text{C}$ . Devices with tall, narrow peaks near  $0^{\circ}\text{C}$  exhibit high precision and low variability. Combined analysis of measurement error distributions (Figure 5) and standard deviation across all temperature steps (Figure 6) confirms generally low noise, with only slightly elevated variability at the temperature extremes and minor, non-linear behavior leading to small but discernible systematic errors. The individual DUT results for both heating and cooling cycles (Figure 6) further demonstrate that this variability is consistent across all devices and does not indicate any systematic temperature-dependent bias.

Collectively, these findings demonstrate the TempVue 20's high precision, stability, and robustness, underscoring its suitability for accurate and reliable temperature monitoring across a broad operational range.